ISSN 2075-1087, Gyroscopy and Navigation, 2024, Vol. 15, No.1, pp. 12-30
Russian Text © The Author(s), 2024, published in Giroskopiya i Navigatsiya, 2024, No.1, pp.15–40

Comparison of Wiener and Kalman Approaches to Marine Gravimetric Survey Data Processing

A. V. Sokolov[a], O. A. Stepanov[a,b,*], A. V. Motorin[a, b], and A. A. Krasnov[a]

[a]*Concern CSRI Elektropribor, JSC, St. Petersburg, Russia*
[b]*ITMO University, St. Petersburg, Russia*
***e-mail: soalax@mail.ru*
Received: March 11, 2024; reviewed: April 9, 2024; accepted: April 10, 2024

Abstract: The paper considers the interrelation, distinctions and features of algorithms for processing the results of marine scalar gravimetric survey, synthesized within the Kalman and Wiener approaches. Their advantages and disadvantages in solving the problems of filtering and smoothing are analyzed. The authors present and compare the results obtained with various recursive filters in simulation and real data processing. The consistency of filters and the possibility to create their adaptive versions suggesting, among other things, the identification of signal and noise models, are discussed.

Keywords: gravimetric survey, Wiener filter, Kalman filter, filtering, smoothing, gravity anomaly, comparison, accuracy.

1. INTRODUCTION

It is a common knowledge that one of the challenges during a gravimetric survey on a moving vehicle is the need to separate the inertial and gravitational components of the specific force measured by the gravimeter [1–7]. Currently, it is common practice to distinguish between the problems of vector gravimetry where the full vector of gravity disturbance (GD) is determined as the difference between the gravity vector and the normal gravity vector at the measurement point, and the problems of scalar gravimetry which determines the gravity anomaly (GA) depending on the value of the GD vector along the true vertical [6–9]. Separation of inertial and gravitational components during a scalar gravimetric survey, as a matter of fact, consists in estimating (isolating) the useful signal of the GA against the background of inertial noise and measurement errors. A strict mathematical statement of this problem for the scalar gravimetric survey on a moving vehicle can be formulated on the assumption that all the components of the signal measured by the gravimeter, including the GA, vehicle's inertial acceleration, and measurement errors, are random processes. A traditional solution to the problem of the useful signal estimation is aimed at the estimation error variance minimization, and the estimates obtained in this solution are called optimal in the root-mean-square (RMS) sense. This problem is solved using two approaches. One of them assumes that the random processes are stationary, and they are described with spectral densities or correlation functions [10–14]. In the other approach, non-stationary processes are generally described in the time domain, using the forming filters represented as differential equations [14–19].

In the first approach, the most widespread solution of the estimation problem is found for stationary processes in steady-state mode. This approach was used by N. Wiener [10] and is often called the Wiener, or frequency-based, approach. As a result, stationary filters are synthesized, which are optimal for the steady-state mode (with infinite time). These filters ensure the calculation of optimal estimates and are specified by transfer functions (TF), frequency response or weight functions [10–14]. They are widely used in solving various applied problems, and it is these filters that have been called the Wiener filters (WF) in the field of engineering. This term will be further used in this sense in this paper.

In the second method called the Kalman approach, the synthesized filters provide optimal estimates which minimize the variance of their errors both in the steady-state mode and during the transient process within a limited time interval. Therefore, in contrast to the first approach, the resulting filters are nonstationary even if the processes themselves are stationary. Furthermore, these filters can also be used in solving the estimation problems for nonstationary processes with finite time, but in this case there will be some

limitations due to the Markovian type of the processes being estimated. These filters known as the Kalman filters (KF) or the Kalman-Bucy filters are set in the time domain, using differential or difference equations [14–22]. In this context we will use the term Kalman filter hereinafter. It would be fair to say that Kalman-Stratanovich is a more correct term for the Kalman approach and the Kalman filter, since the algorithm described in the work by Kalman and Bucy was published by R.L. Stratanovich [23, 24] before the work [15] publication. However, in view of the existing tradition, we will further call them the Kalman approach and the Kalman filter.

Note that when estimating the signals within the stochastic approach, filtering and smoothing tasks are usually considered separately. In the filtering problem, the estimate is found in real time, using only the measurements that are available at the moment. In the smoothing problem, all available measurements are involved, and this estimate is found in the post-processing mode. The filters intended for solving the problems of smoothing are called the smoothers [25–28]. Since there is no requirement for obtaining the estimates at the current time point during a gravimetric survey on a tack, the processing algorithms can be formed using all accumulated measurements, so the smoothers can be applied successfully, and this is what actively implemented in practice.

It is important to emphasize that the optimality should be correlated with the models of processes describing the GA, inertial accelerations and the errors of their measurements, for which these filters have been synthesized. Obviously, the Kalman filter in steady-state mode and the Wiener filter should coincide for the same models, because they are used for minimizing the same criterion. The differences consist only in the form of representation: differential equations for the KF, or TF, weight function or frequency response for the WF.

It should be noted that modern gravimetric surveys can be carried out from both aircraft (airborne gravimetry) and sea vessels (marine gravimetry) [6, 7, 20, 29–40].

Marine gravimetric surveys [6, 29–33, 41–49] have a much longer history than the surveys from aircraft [7, 20, 34–40, 50]. When the marine gravimetric surveys were already in active progress, the Kalman filtering methods were just at the conception stage, and the computing capabilities for their implementation were limited. It is these circumstances that explain the fact that the Wiener approach and corresponding stationary filters have become most popular in constructing the algorithms for marine survey data processing in practice [6, 29–33, 41–45].

By the time it was necessary to implement the methods for processing the airborne gravimetric survey data, the Kalman filtering algorithms and computing tools had developed significantly. In addition, the solution of filtering problem itself became noticeably more complicated and required the use of external meters to effectively compensate for inertial interference, since their frequency spectrum was close to that of the GA due to the high speed of aircraft. These circumstances were good prerequisites for active application of the Kalman filtering algorithms in airborne gravimetry, which has been actually implemented in practice [20, 35–40].

Based on the above, it is essential to compare the advantages and disadvantages of the Wiener and Kalman filtering methods as applied to marine gravimetric surveys.

The purpose of this work is to discuss the interrelations, differences and features of algorithms for processing the marine scalar gravimetric survey data, synthesized within the framework of Kalman and Wiener approaches, and to analyze their advantages and disadvantages.

It should be noted that the question of correlation of filtering algorithms synthesized within the two approaches and used, among other things, for solving a wide range of problems of navigation information processing, was previously discussed in the literature [14, 19, 21, 51–53]. The authors believe that the proposed work is of interest in this sense, too, since it concerns the correlation of algorithms as applied to the problem of scalar gravimetric survey data processing. The subject under study has already been touched upon in [54–56], and the proposed work develops this issue.

We also draw attention to the fact that in this paper the problem of the GA estimation using measurements accumulated on the tack is solved. A more general task is to determine the GA based on the results of 2D (areal) survey for mapping purposes [6, 57, 58], in particular, by estimating the spatial field represented by orthogonal expansion with unknown coefficients [6, 57]. The specific features of this problem are beyond the scope of this work and are worth discussing in a separate study.

The paper is structured as follows. After the introduction, the first section describes the models of GA

and vertical motion, used in the work, and provides a related mathematical model of measurements with a damped gravimeter. In the second section, based on these models, the algorithms for the GA filtering and smoothing are formulated and described, first in the time domain from the standpoint of the Kalman (time-based) approach without simplifications, and then from the standpoint of the Wiener (frequency-based) approach, using the method of local approximations (MLA). In the third section, the TF, weight functions and amplitude-frequency response characteristics (frequency response hereinafter) are constructed and compared for the stationary filters corresponding to the KF in steady-state mode, the WF, and a stationary filter often used in practice. Characteristics of filters, such as cutoff frequency, bandwidth, and spatial resolution, as well as the specifics of their definition with regard to the KF are also discussed in this section. In the fourth section, the results of the GA estimation using the described algorithms, modeled and actual data are presented and compared. The main results are summarized in the conclusions.

2. MODELS OF USEFUL SIGNAL, INTERFERENCE AND GRAVIMETRIC MEASUREMENTS

As was mentioned in the introduction, the task under consideration consists in isolating the GA against the background of inertial accelerations of a moving object from which the survey is being carried out. Assuming that the gravimeter measurements are the sum of uncorrelated random processes describing the GA useful signal g_a and the interference (inertial vertical accelerations) $\ddot{h}$, we present them first in the form [1–7]:

$$y^* = g_a + \ddot{h}. \tag{1}$$

Regardless of the approach used, in order to build optimal filters, it is necessary to set the stochastic models of the useful signal and interference. In this case, we will use the models in the state space for the Kalman formulation, and the models in the form of correlation functions or spectral densities for the Wiener formulation. Now we will describe the models of GA and vertical motion of an object, used in this work, and touch on the features of obtaining the measurements in the form of (1) according to the data of a damped gravimeter.

2.1 GA Model

To describe the GA, we will use the Jordan model. In the state space, this model can be represented as follows [59]:

$$\begin{aligned} \dot{x}_1 &= -\beta x_1 + x_2, \\ \dot{x}_2 &= -\beta x_2 + x_3, \\ \dot{x}_3 &= -\beta x_3 + w_{ga}, \\ g_a &= -\beta\zeta x_1 + x_2, \end{aligned} \tag{2}$$

where $\beta = V\sigma_{dga}/\sqrt{2}\sigma_{ga}$; V is the motion speed; σ_{ga} is the GA standard deviation; σ_{dga} is the standard deviation of the GA derivative with respect to the trajectory length; w_{ga} is generating white noise with intensity $10\beta^3\sigma_{ga}^2$, $\zeta = (\sqrt{5}-1)/\sqrt{5}$. The GA spectral density corresponding to this model is defined by the following formula:

$$S_{ga}(\omega) = \frac{2\beta^3\sigma_{ga}^2\left(5\omega^2+\beta^2\right)}{\left(\omega^2+\beta^2\right)^3}. \tag{3}$$

2.2. Vehicle's Vertical Motion Model

It is advisable to describe the vertical accelerations of a vehicle in the state space in accordance with other parameters of its vertical motion, namely, its vertical displacements and velocities. To describe the vertical accelerations, velocities, and displacements of an object, we will use the model from [60]:

$$\begin{aligned} \dot{x}_4 &= x_5, \\ \dot{x}_5 &= x_6, \\ \dot{x}_6 &= -a_3x_4 - a_2x_5 - a_1x_6 + w_h, \end{aligned} \tag{4}$$

where $x_4 = \Delta h$ is the vehicle's vertical displacement above the reference ellipsoid with the standard deviation equal to $\sigma_{\Delta h}$; $x_5 = \dot{h}$, $x_6 = \ddot{h}$ are the vertical velocity and acceleration. The coefficients included in (4) are defined as $a_3 = \left(\lambda^2+\mu^2\right)\gamma$, $a_2 = \lambda^2+\mu^2+2\mu\gamma$, $a_1 = 2\mu+\gamma$, where $\lambda = 2\pi/T$, T is the dominating period of vertical accelerations; μ is the coefficient of vertical accelerations non-uniformity; γ is the coefficient set for the model compliance with the selected characteristics of the sea waves. The generating white noise intensity w_h is set by the value of $2\sigma_{\Delta h}^2 a_3\left(a_1a_2-a_3\right)/a_1$. Standard deviations of vertical displacements $\sigma_{\Delta h}$ and $\sigma_{\dot{h}}$ are related as $\sigma_{\dot{h}} = \sigma_{\Delta h}\sqrt{(a_2a_3)/a_1}$. To implement the Wiener approach, it is sufficient to know the spectral density of

vertical accelerations. It can be shown that the spectral density of vertical accelerations, corresponding to this model is defined as follows:

$$S_{\ddot{h}}(\omega) = \frac{2\sigma_{\ddot{h}}^2}{a_2} \frac{\omega^4 (a_1 a_2 - a_3)}{\omega^6 + (a_1 - 2a_2)\omega^4 + (a_2^2 - 2a_3 a_1)\omega^2 + a_3^2}. \quad (5)$$

2.3 Model of Measurements with Damped Gravimeter

The representation of measurements in the form of (1) is some approximation. When taking measurements, it is necessary to allow for the values of normal gravity and its variation along the motion trajectory, the accelerations caused by the Eotvos and Harrison effects, the orbital effect, etc. [6]. In addition, the gravimeters used on moving objects are relative, so it is also necessary to know the GA values at the reference point in order to determine the GA. These allowances can be calculated by known relationships and taken into account in the gravimeter measurements as appropriate.

Note that damped gravimeters are primarily used in marine gravimetry [29, 42–45, 58, 61]. They are distinctive in that their sensitive element is an elastic pendulum suspended in a damping liquid. This helps to additionally dampen the high-frequency vertical accelerations of the vehicle, but makes the measurement formation process more specific. Within the framework of the Kalman approach, the above features can be taken into account by representing the gravimeter readings y in the following form:

$$\dot{x}_7 = -\frac{1}{T_g} x_7 + \frac{1}{T_g}\left(g_a + \ddot{h}\right) + \frac{1}{T_g}\Delta g, \quad (6)$$

$$y = x_7 + v_g, \quad (7)$$

where x_7 is the gravity increments relative to the reference point, T_g is the time constant of the gravimeter, v_g is the instrumental white-noise error of gravimeter with intensity r^2, Δg is the sum of accelerations caused by the Eotvos and Harrison effects, the orbital effect, and the normal gravity variations along the trajectory [6, 58, 61].

When synthesizing the algorithms within the framework of the Wiener approach, the specificity of the damped gravimeter is taken into account by applying a special recovery procedure consisting in numerical differentiation of the gravimeter readings [6, 58, 61]. As a result, after compensating for the listed allowances, a measurement model in the form of (1) can be used.

3. GA ESTIMATION: PROBLEM STATEMENT AND SOLUTION ALGORITHMS

Let us formulate two statements of the GA estimation problem—Wiener and Kalman ones—and briefly discuss the filtering and smoothing algorithms that follow from them.

4.1 Kalman Problem Statement. Kalman Filter and Kalman Smoother

The Kalman problem statement consists in the state vector estimation:

$$\begin{aligned}
\dot{x}_1 &= -\beta x_1 + x_2,\\
\dot{x}_2 &= -\beta x_2 + x_3,\\
\dot{x}_3 &= -\beta x_3 + w_{ga},\\
\dot{x}_4 &= x_5,\\
\dot{x}_5 &= x_6,\\
\dot{x}_6 &= -a_3 x_4 - a_2 x_5 - a_1 x_6 + w_h,\\
\dot{x}_7 &= -\frac{1}{T_g} x_7 - \frac{1}{T_g}(\beta\zeta x_1 - x_2 + x_6) - \frac{1}{T_g}\Delta\tilde{g} + \frac{1}{T_g} w_\Delta,
\end{aligned} \quad (8)$$

according to measurements (7).

In (8), $x_i, i = \overline{1.7}$ correspond to models (2), (4), (6), and Δg in Eq. (6) is replaced with $\Delta g = \Delta\tilde{g} - w_\Delta$, where $\Delta\tilde{g}$ is the calculated values of allowances, including the allowances for the Eotvos and Harrison effects, the orbital effect, as well as the variations of normal gravity values along the trajectory, and w_Δ is the error in their calculation. The main contribution in this error is made by the error in calculating the allowance for Eotvos effect in accordance with the data from satellite navigation systems (GNSS). For the sake of simplification, we will further assume that w_Δ is white noise.

For the formulated problem statement, an equation for the KF can be obtained easily, using standard expressions [15–19]:

$$\dot{\hat{x}} = \left(F - K(t)\ H\right)\hat{x} + K(t)\ y + B\Delta\tilde{g}, \quad (9)$$

in which the matrix determining the gain factor $K(t) = r^{-2} P(t) H^T$, the matrices of dynamics F, control B, observation H, and measurement noise intensity r^2 correspond to the set of equations (8) and the model of measurements (7), while the estimation error co-

variance matrix $P(t)$ is found by solving the Riccati differential equation

$$\dot{P} = FP + PF^T + GQG^T - r^{-2}PH^THP. \qquad (10)$$

The matrix of generating noises G and the matrix of their intensities Q, included in this equation also correspond to the set of equations (8).

Note that even with unchanged values of the matrices included in the Riccati equation, the matrix $K(t)$ will not be constant, which determines the nonstationary form of the KF even when estimating stationary processes. At the same time, in the steady-state mode, the KF is a stationary filter defined by the equation

$$\dot{\hat{x}} = \left(F - K_\infty H\right)\hat{x} + K_\infty y + B\Delta\tilde{g}, \qquad (11)$$

where $K_\infty = r^{-2}P_\infty H^T$ is a constant matrix defining the gain factor and calculated using matrix P_∞ defining the filtering error in the steady-state mode, satisfying the algebraic Riccati equation:

$$FP_\infty + P_\infty F^T + GQG^T - r^{-2}P_\infty H^T HP_\infty = 0. \qquad (12)$$

To construct a Kalman smoother (KS), a well-known procedure that processes in reverse time the estimates obtained using the KF for all components of the state vector (Rauch-Tung-Striebel smoother) [25–28] can be applied.

Using know relationships, we can obtain a stochastically equivalent discrete statement of the state vector estimation problem (8) based on measurements (7); after that, recursive relationships of the KF and respective recursive relationships of the KS are implemented for estimates calculation.

It is easy to see that the solution of the problem within the framework of the Kalman approach without accounting for the specifics of the damped gravimeter can be easily obtained if we take into account that in this case the filtering problem is solved for the reduced state vector $x_i, i = \overline{1.6}$ from (8), according to measurements (1), where $g_a = -\beta\zeta x_1 + x_2$ and $\ddot{h} = x_6$. Here, the white-noise error of the gravimeter, which does not significantly affect the result, can be added directly to measurements (1).

Wiener Problem Statement. Wiener Filter and Wiener Smoother

When solving the problem within the Wiener formulation, we will assume that the gravimeter measurements are described by model (1) in which the signal (GA) and interference (vertical accelerations) are specified by spectral densities (3) and (5), respectively. It is required to obtain a GA estimate, using measurements (1) and information about the spectral density (3), (5). As a result, separation and factorization procedures make it possible to find the corresponding TF for the WF and Wiener smoother (WS) [12, 13]. In this case, the smoother is implemented by forward-time processing of the measurements and subsequent processing of the obtained estimates in reverse time.

For sufficiently complex models (3), (5), the process of TF derivation is not trivial; in practice, the MLA of spectral densities proposed in the works by I.B. Chelpanov and L.P. Nesenyuk [12, 13] and the time-frequency approach developed on its basis for the construction of filtering and smoothing algorithms has been widely used [52, 62]. The idea of this method consists in combined application of the Kalman and Wiener approaches, including MLA.

According to the MLA, when solving the problem under consideration, the spectral densities of GA and those of vertical accelerations are approximated as follows:

$$S_{ga}(\omega) \approx r_\varepsilon^2 \frac{\omega_c^4}{\omega^4}, \qquad (13)$$

$$S_{\ddot{h}}(\omega) \approx r_\varepsilon^2 \frac{\omega^4}{\omega_c^4}, \qquad (14)$$

where r_ε^2, ω_c^4 are the values of the spectral density and the frequency of the intersection point of the approximated spectral densities of the signal and interference (Fig. 1). In this case, the parameters of the TF that determines the corresponding WF for the useful signal (13) estimation against the background of interference (14) depend on the intersection point of their spectral densities.

Applying the models (13), (14) arising from the MLA, it can be shown [62] that the TF for the WF in the GA filtering problem has the form

$$H_y^{g_a}(p) = \frac{\alpha_B\omega_c^3 p + \omega_c^4}{p^4 + \alpha_B\omega_c p^3 + 0.5\alpha_B^2\omega_c^2 p^2 + \alpha_B\omega_c^3 p + \omega_c^4}, \qquad (15)$$

where $\alpha_B = \sqrt{2}\sqrt{2+\sqrt{2}} \approx 2.613$; $\omega_c = 2\pi f_c$ corresponds to the signal and interference intersection point (Fig. 1).

The TF corresponding to the solution of the GA estimation problem in the smoothing mode, i.e., obtaining a smoothed estimate has the form:

$$H_y^{g_a^s}(p) = \frac{\omega_c^8}{p^8 + \omega_c^8}. \qquad (16)$$

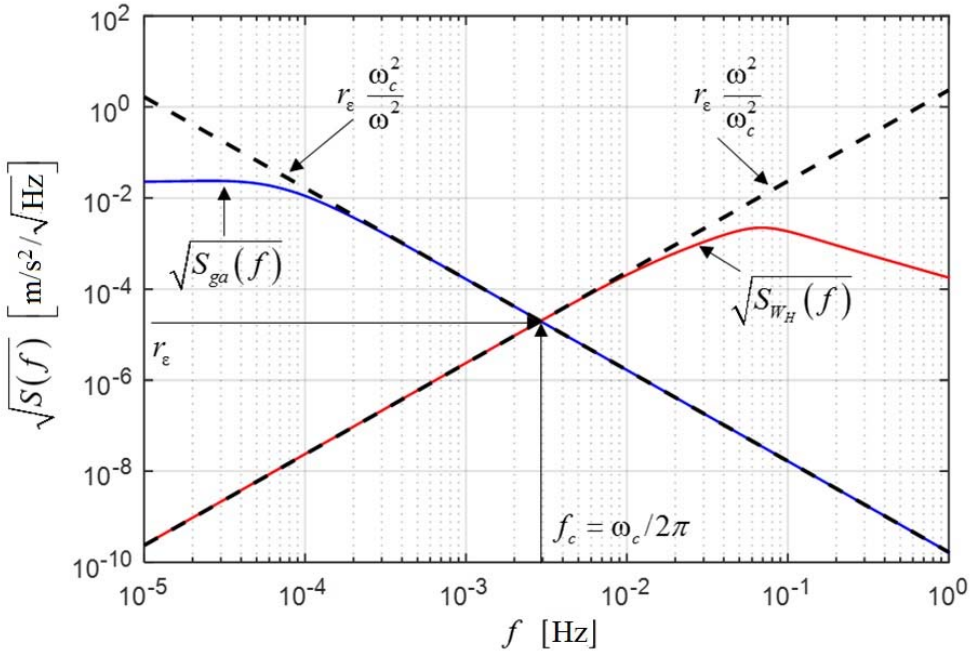

Fig. 1. Square roots of spectral densities of GA and vertical accelerations (solid lines), and their approximations (dotted lines).

To calculate the desired smoothed estimate, it is sufficient to process the measurements of specific force (1) in forward time and the resulting estimates in reverse time, using a filter with TF corresponding to the Butterworth filter of the 4th order with a cutoff frequency ω_c:

$$H_y^{g_a^s}(p) = \\ = \frac{\omega_c^4}{p^4 + \alpha_B\omega_c p^3 + 0.5\alpha_B^2\omega_c^2 p^2 + \alpha_B\omega_c^3 p + \omega_c^4}. \quad (16)$$

The fact that the resulting TF corresponds to (16) after such processing can be easily verified by multiplying the TF (17) by a complex conjugate function [31].

Note that the TF for the optimal filter (15) and the TF (17) for the smoother are different. Curiously, the filter with TF (17) does not provide an optimal solution to the filtering problem when processing the measurements in forward time, while the filter with TF (15) does not provide an optimal solution to the GA smoothing problem for models (13), (14) when processing the implementation in forward time and the obtained estimates in reverse time. Without dwelling on the details of relationship and differences of the TF used in filtering and smoothing within the Wiener approach, we should only mention that it has been considered in [19, 26].

One should bear in mind that the WF and WS obtained using MLA will be suboptimal with respect to models (3), (5) and their corresponding KF and KS when estimating the state vector (8) by measurements (7) in steady-state mode. This is due to the fact that they were constructed using the approximation of signal and interference spectral densities, the presence of gravimeter errors and errors in calculating the corrections w_Δ was neglected, and the specific procedure of signal recovery was not taken into account.

It should be noted that within the Wiener approach, the calculated values of the root-mean-square error (RMSE) of the GA estimation can be obtained based on the condition of the error variance finiteness, as well as using the time-frequency approach discussed below [62]. For the WF (15) constructed for simplified models (13), (14), standard deviation can be calculated as follows [62]:

$$\sigma_f(g_a) = r_\varepsilon \sqrt{\frac{\omega_c}{\left(1.5-\sqrt{2}\right)\sqrt{2+\sqrt{2}}}} \approx 2.51 r_\varepsilon \sqrt{\omega_c},$$

and for the WS (16), (17) — as

$$\sigma_s(g_a) = \frac{r_\varepsilon}{2} \sqrt{\frac{\omega_c}{\sqrt{2+\sqrt{2}}}} \approx 0.37 r_\varepsilon \sqrt{\omega_c}. \quad (17)$$

It follows from the presented relationships that the standard deviation of the GA smoothing is almost 7 times less than that of filtering.

Note 1. It should be noted that the above problem statements for the GA estimation do not provide for availability and some consideration of high-precision measurements of the altitude and/or vertical velocity of the moving object, as is done in airborne gravime-

try. The possibility to consider the problem in this way when measuring the GA from moving marine vehicles is based on the fact that the latter have a lower speed compared to aircraft, and as a result, a different frequency composition of the useful signal and interference. This creates prerequisites for achieving acceptable accuracy of the GA estimation in sea conditions without involving any additional measurements. This can be done by filtering (smoothing) to suppress the interference, while the useful signal distortion will be minimal. On aircraft, the spectra of useful signal and vertical accelerations significantly overlap due to its high speed, and the attempts to achieve the required accuracy of the GA estimation at the background of this interference fail. For this reason, additional high-precision measurements of the vehicle's vertical displacements, obtained from GNSS have to be used. As a result, the problem is solved in the formulation that is invariant with respect to the vertical acceleration, which is achieved by forming the differential measurements of the gravimeter and GNSS. Essentially, on the aircraft the same useful signal (GA) is estimated against the background of other interference, i.e., the GNSS errors.

At the same time, it is clear that the estimation problem can also be generalized with respect to a marine object in case the high-precision measurements from GNSS are involved. For this purpose, in the Kalman formulation, appropriate additional measurements should be added in (7). Some results of studies on the effectiveness of high-precision GNSS measurements use in marine gravimetric surveys are presented in [63, 64]. Since in this case we are talking about the study of systems with many inputs, i.e., gravimeter and GNSS measurements, preference should be given to the Kalman approach, since it is suits better for processing such measurements.

Note 2. The cases considered above relate to scalar gravimetry, i.e. the GA estimation, and in this paper, the gravimeter measurements are understood as the measurements of a gimbaled scalar gravimeter [6, 41–50, 61, 63]. On the other hand, when constructing strapdown inertial scalar gravimeters [7, 65, 66], GA measurements can be obtained using the data from strapdown inertial systems (SINS) by converting signals from a triad of accelerometers rigidly fixed on the base, taking into account the object attitude angles calculated according to the SINS algorithms. The Kalman approach has become widespread in these systems, in particular, for correcting the SINS errors [7]. This scheme can also be used in vector gravimetry, i.e., for obtaining the estimates of the full GD vector, since the SINS algorithms generate both vertical and horizontal components of accelerations. It is stated in [7] that a strapdown inertial gravimetric system and a SINS integrated with GNSS are almost identical in terms of equipment composition. The differences are only in the requirements for the accuracy of inertial sensing elements, knowledge of the Earth's gravity field, and the composition and accuracy of GNSS receivers. In this sense, a scalar gravimeter is actually a vertical channel of a strapdown inertial gravimetric system.

4. COMPARISON OF THE KALMAN AND WIENER APPROACHES

When analyzing the effectiveness of Kalman-type filters, the emphasis is usually made on the values of the RMSE and the transition time, which are actually minimized for the selected models of the estimated signal and measurement errors. On the other hand, when analyzing the properties of stationary filters represented by TF, in addition to the RMSE, the type of frequency response corresponding to them and the parameters calculated using it, such as cutoff frequency, bandwidth and resolution, are usually discussed. Since the KF is a stationary filter in steady-state mode, it is advisable to form and calculate these parameters for the KF, and to use them when considering the properties and comparing the resulting algorithms.

It is clear that in case of the same models, comparison of the KF in steady-state mode and the WF is out of question, because, as was already mentioned in the introduction, these filters coincide with each other. The specific features can only manifest themselves depending on whether a filter is implemented based on an expression using a TF, a weight function or frequency response, or on its representations using linear stationary equations. These features, in particular, may be the result of ambiguous transition from the representation of a dynamic system (a filter in this case) using a TF to its representation using the state space. Nevertheless, these features do not have any effect on the properties of stationary filters. It is pertinent to note here that the KF in steady-state mode represents a WF, and vice versa, a WF can be considered as a Kalman-type filter with a constant gain coefficient.

As was shown above, the WF can be constructed using MLA. In addition, in practice, when processing the marine gravimetric survey results, a stationary

filter (SF) is often used, which is a series of the fourth-order Butterworth filter and an aperiodic link with the resulting TF [6, 58, 61]:

$$H_y^{g_a}(p) = \frac{\omega_a}{p+\omega_a}\frac{\omega_b^4}{p^4+\alpha_B\omega_b p^3+0,5\alpha_B^2\omega_b^2 p^2+\alpha_B\omega_b^3 p+\omega_b^4}, \quad (18)$$

where $\omega_a = 1/T_a$; $\omega_b = 2\pi/T_b$; T_b = 60 s, T_a = 90 s are the time constants of the Butterworth filter and the aperiodic link, respectively [6], which are selected empirically based on the survey conditions.

Thus, it is of interest to compare the characteristics of the KF constructed for complete models; the WF constructed for the models obtained using MLA; and the stationary filter (SF) constructed from empirical considerations. A brief description of the algorithms compared is summarized in Table 1 for convenience.

Table 1

Brief description of filters and smoothers under comparison

Filters	Smoothers
KF: Kalman filter set for model (8) and measurements (7)	**KS:** A smoother implemented by processing measurements in forward time using the KF and the obtained estimates of the state vector (8) in reverse time according to [25].
WF: Wiener filter set for the model of useful signal and interference (13), (14) with TF (15)	**WS:** Smoother with TF (16), implemented by processing the measurements in forward time and the received GA estimates in reverse time, using a filter with TF (17).
SF: Stationary filter with TF (20)	**SS:** A stationary smoother implemented by processing the measurements in forward time and the obtained GA indirect estimates in reverse time, using a filter with TF (20).

Further in this section, we will study and compare the frequency response and the weight functions of the KF in steady-state mode, the WF, and the SF discussed above.

The desired frequency response for the KF in steady-state mode can be obtained using a TF that links measurements (1) with the GA estimate in the KF, and has the form [19]:

$$W_y^{g_a}(p) = D\left(pE - F + K_\infty H\right)^{-1} K_\infty, \quad (19)$$

where K_∞ satisfies (11), and $D = \left[-\beta\zeta \;\; 1 \;\; 0 \;\; 0 \;\; 0 \;\; 0\right]$, because $g_a = Dx$. The problem of obtaining TF (21) in an analytical form is reduced to the need to get an analytical solution to the Riccati equation (12) in order to calculate P_∞ and then to define K_∞, which is generally quite difficult. However, the matrix K_∞ determining the gain coefficient of the KF in steady-state mode can be obtained from the numerical solution of the Riccati equation (12) for particular values of the initial data, after which it can be used for constructing the desired frequency response (21).

In order to compare the frequency responses, the TF was calculated for the KF in steady–state mode (21) with the following values: standard deviation of GA variability σ_{dga} = 3 mGal/km; standard deviation of GA σ_{ga} = 30 mGal; standard deviation of vertical accelerations $\sigma_{\dot{h}}$ = 10 Gal; period T = 5 s; non-uniformity μ = 0.05 s^{-1}; motion speed V = 10 kt; RMSE of gravimeter's measurements 0.5 mGal; sampling frequency 10 Hz. The corresponding frequency response is shown in Fig. 2. For comparison, the frequency response of the WF with TF (15) obtained using MLA for the corresponding local approximations is also shown in the figure.

The frequency response (Fig. 2) and weight functions (Fig. 3) corresponding to the KF in steady-state mode with TF (21), the WF for simplified models with TF (15), and the SF with TF (20) were obtained in the MatLab software, using built-in functions.

Analyzing the type of frequency response (Fig. 2), it can be noted that the KF and WF are low-pass filters, and they almost coincide in the frequency response bandwidth. As we can remember, the bandwidth (transparency) or effectively transmitted frequency band is a frequency range within which the frequency response of the filter can be considered uniform and ensures signal transmission without significant distortion. The cutoff frequency is the frequency for which the frequency response level is halved compared to the value in the bandwidth [67]. Therefore, the frequency response at the cutoff frequency has a decrease to lg2≈0.707 (or approximately –3 dB) relative to the level in the bandwidth. The cutoff frequency serves as an empirical boundary of the filter bandwidth and also characterizes the spatial resolution of the marine gravimetric survey as discussed below. Note that the cutoff frequency for the WF (15) depends only on $\omega_c = 2\pi f_c$, i.e., the frequency of the intersection point of the spectral densities of the signal and interference, and for the KF it is determined by all

the parameters of the models used. The differences in frequency responses of the KF and WF in the suppression band (Fig. 2) are caused by the differences in spectral densities of interference.

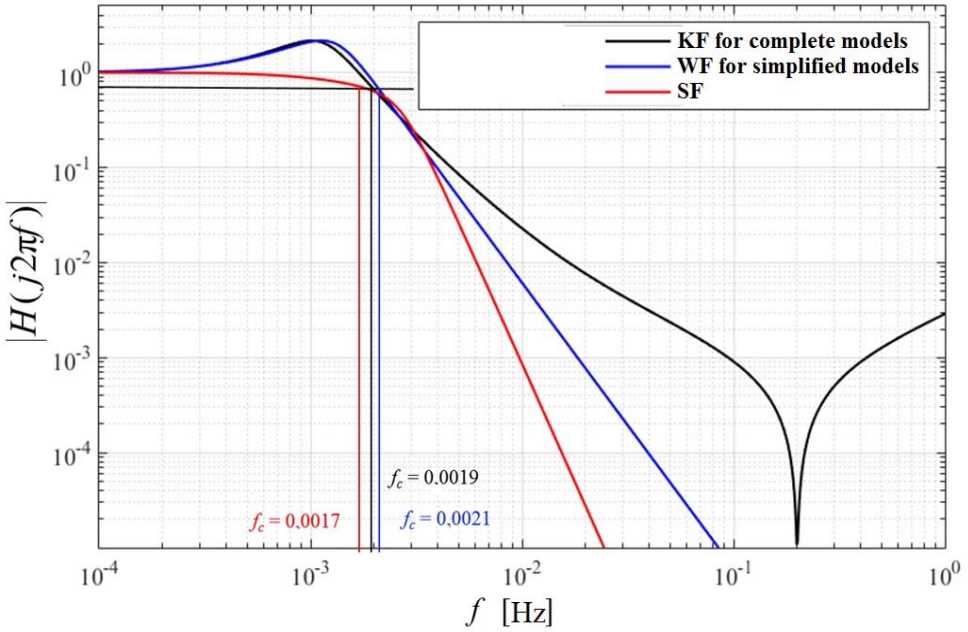

Fig. 2. Amplitude-frequency response of the KF, WF and SF.

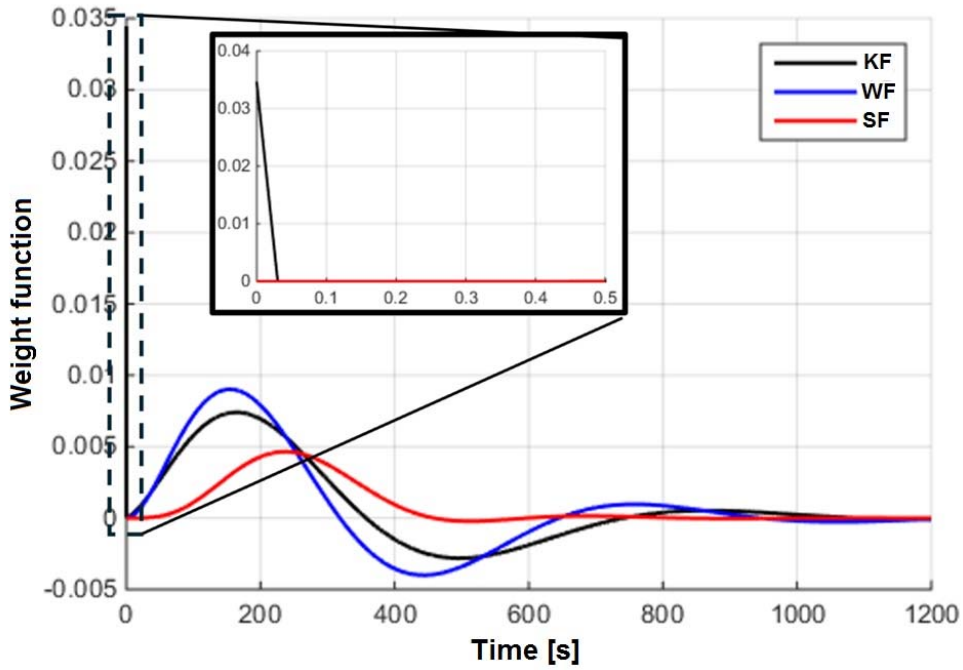

Fig. 3. Weight functions of the KF, WF, and SF.

Thus, as expected, the considered KF and WF have similar frequency responses and weight functions (Fig. 3). However, the weight function of the KF has larger values at zero time, which corresponds to frequency response increase in the frequency range above 0.2 Hz. These functions are also similar in many ways to the frequency response and weight functions of the SF with TF of type (20), used in practice. Nevertheless, in the case of SF, the choice of a particular type of frequency response and/or weight function usually depends on empirical considerations about the nature of the estimate obtained, while in the case of the KF and WF, the choice of the filter weight function depends on the parameters set for the stochastic models of the signal and interference.

When estimating the GA, the characteristic of spatial resolution is also taken into consideration along with the RMSE. The term "resolution" is used in various fields as a characteristic reflecting the possibility to distinguish fine details of useful signal in the data obtained after processing with a certain algorithm. In gravimetry, the resolution is usually defined as a half of the GA minimum wavelength ρ that can be high-

lighted on a map or profile [68–70]. When processing the data from marine or airborne gravimetric survey, the value of ρ depends on the cutoff frequency of the filter used and on the vehicle's speed [70]:

$$\rho = \frac{V}{2f_c}, \tag{20}$$

where ρ is half of the minimum wavelength distinguished in the GA (m); V is the vehicle's speed (m/s); f_c is the cutoff frequency of the filter used for the data processing (Hz). The smaller the minimum wavelength ρ, the higher the spatial resolution. As was mentioned earlier, the cutoff frequency for the KF and WF under study is determined by the stochastic models of GA and vertical accelerations.

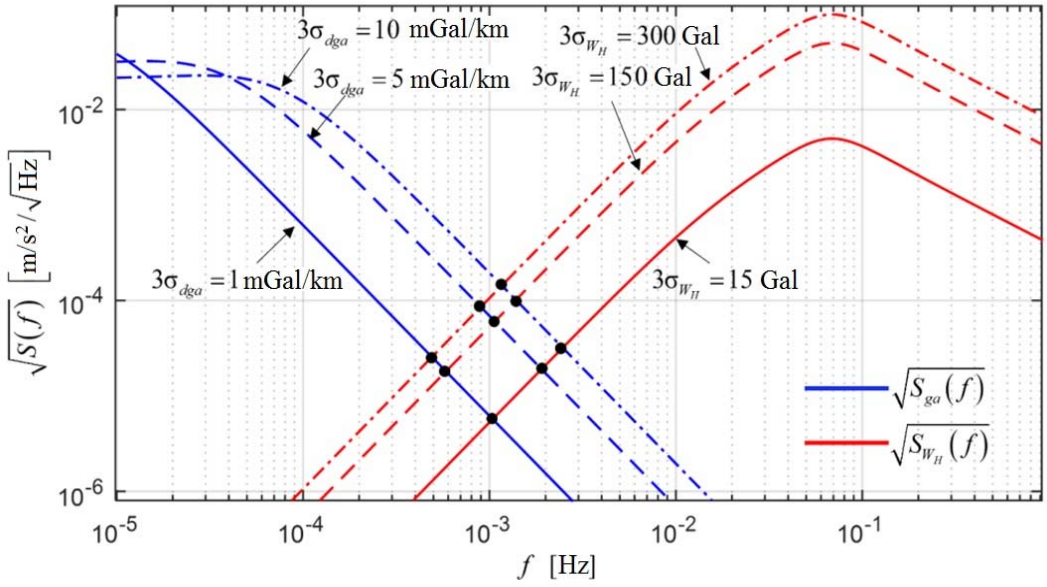

Fig. 4. Graphs of square roots of the GA spectral densities and vertical accelerations.

It follows from Fig. 4 that with an increase in the GA variability (gradient) under the same survey conditions (i.e., with the same vertical accelerations), on the one hand, the RMSE of the GA estimation increases, and on the other hand, the spatial resolution becomes higher. This seemingly contradictory statement is based on the fact that with increasing variability of the GA, the level of its high-frequency components that can be better distinguished against the background of the same vertical accelerations increases, too. In this case, the accuracy of the GA estimation decreases. At the same time, with constant variability and increasing level of vertical accelerations, the RMSE of the GA estimation will also increase, while the spatial resolution will degrade. Thus, it can be stated that the spatial resolution depends on the survey conditions described by the corresponding models of GA and vertical accelerations.

It is certainly an interesting question: what are the models presented in the state space for the useful signal and interference? In our case, these are the models for the GA and vertical motion, that have formed the TF corresponding to one or another SF. Generally speaking, this question is difficult to answer. It should be noted that it is quite easy to construct a model with a constant gain coefficient in the state space for a given TF defining one or another SF, and, as is known, this model is not the only one. However, which models for a useful signal have resulted in such a TF is still an open question. It turns out that the answer to this question can be obtained for simplified models (13), (14) within the framework of the time-frequency approach. Let us explain how to do this based on the works [12, 13, 52, 62]. To this end, we introduce a forming filter (FF) for the simplified GA model in the form [62]:

$$\begin{aligned} \dot{g}_1 &= g_2, \\ \dot{g}_2 &= w, \\ g_a &= g_1, \end{aligned} \tag{21}$$

where w is a generating white noise with intensity $r_\varepsilon^2\omega_c^4$. Strictly speaking, it is impossible to directly introduce a model in the form of the FF for the interference with spectral density (14), because according to the classical theory, white noise is not a differentiable process. Nevertheless, the problem statement under consideration can be formulated using the concept of a conditional spectral density [46]. By integrating the measurements twice, we reduce this problem to an equivalent (from the point of view of the resulting solution) problem statement for estimating the state vector described as

$$\begin{aligned} \dot{x}_1 &= x_2, \\ \dot{x}_2 &= g_1, \\ \dot{g}_1 &= g_2, \\ \dot{g}_2 &= w, \end{aligned} \tag{22}$$

based on measurements

$$\tilde{y} = x_1 + v, \tag{23}$$

where $\tilde{y}$ is the second integral from measurements (1), v is the white noise of measurements with intensity $r_\varepsilon^2/\omega_c^4$. Formally speaking, these are the measurements of altitude. However, it is shown in [62] that, in terms of obtaining the TF, estimation of GA $g_a = g_1$ described by the FF (22) according to measurements (23) is equivalent to estimation of GA with spectral density (13) against the background of interference with spectral density (14) according to measurements (1), where $g_a = -\beta\zeta x_1 + x_2$. Using these results and the relationship (21), it is not difficult to show that the TF of such KF in the steady-state mode coincides with (15). In addition, it can be shown that the RMSE of estimation in the steady-state mode will coincide with (18).

Taking into account the presented material, we can give the following explanation of the term "time-frequency approach". When obtaining a filter in steady-state mode in the form of TF, the Wiener (frequency-based) approach is applied, which is based on the use of spectral densities. On the other hand, to ensure the filter optimality in the transient mode, a model in the form of differential equations is used, which makes it possible to apply the Kalman approach.

Thus, for the reduced models (13), (14), a KF can be implemented, which in steady-state mode coincides with the stationary WF (15) for the same models. It is important to emphasize that this filter is stationary only in steady-state mode, and during the transient process its gain coefficient changes. It has an important advantage over the WF, since it is the optimal KF for the models (13), (14) and provides optimal estimates not only in steady-state mode, but also in transient mode, in contrast to the WF specified by TF (15). Due to this, the transient process time reduces when such a filter is used.

It is important to mention that in [27] which is also devoted to the a smoother construction, the problem is solved within the Kalman approach for models similar to (24) and (25); the difference is that the GA is described by the third integral of white noise. At the same time, the emphasis is made on constructing a suboptimal smoother. In order to create an algorithm with low computational load, the authors of [27] neglect the generating noise. The relationships between the Kalman and Wiener algorithms are not addressed in this work. Therefore, it can be stated that in contrast to [27], when implementing the smoothing algorithm obtained within the time-frequency approach, the scalar version of the GA estimates is processed in reverse time, which also reduces the amount of computation when constructing the filter.

5. COMPARISON OF THE KALMAN AND WIENER APPROACHES BASED ON THE RESULTS OF SIMULATION AND REAL DATA PROCESSING

To compare the KF and WF, simulation was carried out under the following conditions: standard deviation of vertical accelerations within the range of 2–20 Gal; standard deviation of the GA variability within the range of 1–3 mGalл/km; vertical accelerations period $T = 5$ s and non-uniformity $\mu = 0.05$ s^{-1}, typical of a marine vehicle; speed $V = 10$ kt; white-noise RMSE of gravimeter $\sigma_g = 0.1$ mGal; RMSE of corrections calculation $\sigma_{w\Delta} = 0.5$ mGal; sampling frequency 10 Hz.

The results described in this section were obtained taking into account the above-mentioned features of the damped gravimeter and correction input.

Figure 5 shows typical curves of the true value and estimates of the GA, obtained with the KF, WF and SF under the worst (adopted for simulation) survey conditions in terms of the estimation accuracy: standard deviation of GA variability 3 mGal/km, standard de4viation of vertical accelerations 20 Gal, which corresponds to the maximum wave height of 1 m. Figure 6 shows the corresponding realizations of GA filtering errors for different filters, and the real RMSE calculated as explained below.

It follows from the graphs in Fig. 5 that the estimates obtained with the KF and WF contain high-frequency components. At the same time, it can be seen that the SF estimates have a greater delay than the KF and WF estimates for which the delay is insignificant in this case, and this ultimately causes a larger RMSE of GA estimation with the SF, as shown in Fig. 6.

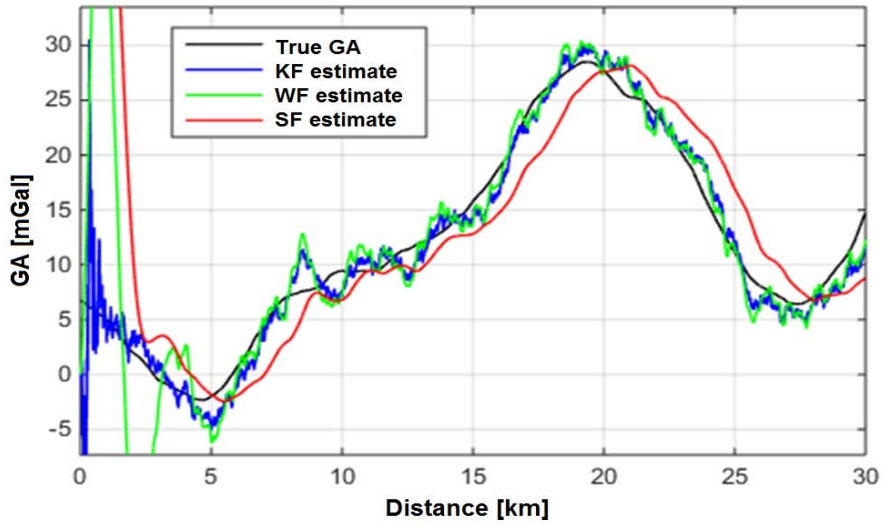

Fig. 5. GA estimates obtained with the KF, WF and SF

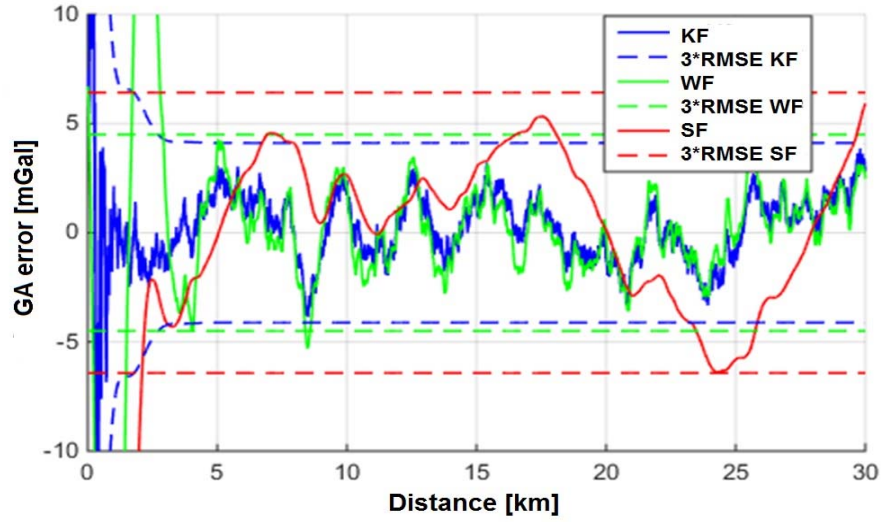

Fig. 6. GA filtering errors for the KF, WF and SF.

Figure 7 shows typical curves of the GA true value and estimates obtained with KS, WS and SS for the same realization of measurements as in Figs. 5, 6. It can be seen that the smoothing mode prevents the phase delay for all filters. Figure 8 presents the errors and the RMSE of the GA estimation for KS, WS and SS. In the simulation, the KS provides optimal estimation accuracy, while the WS constructed using MLA, and the SS are slightly inferior to it in accuracy. Based on this, the following curious fact can be noted: the smoothing mode reduces the effect of accuracy drop when suboptimal filters are used.

At the same time, it should be remembered that the above RMSE for various filters are close to each other only in case of steady-state mode. During the transient process, the errors of the WF and SF are considerably higher than the RMSE of the KF.

Real (r) and calculated (c) RMSE of GA estimation in the steady-state mode were obtained for different survey conditions as summarized in Tables 2, 3. The real and calculated values of the RMSE coincide for the KF and KS set for the original complete models, since GA and vertical accelerations were simulated according to (2), (4). For the WF and WS, the calculated values of RMSE were calculated according to (18), (19), and the real values were calculated according to the statistical test (Monte Carlo) method by modeling a set of realizations and subsequent averaging [71]. For the SF and SS, only real RMSE calculated in the same way are given, since this filter does not imply a calculated accuracy characteristic.

It follows from Table 2 that the real RMSE of the WF and SF are much (up to two times) higher than the real RMSE of the KF. In this situation, the SF shows the greatest RMSE, although its estimates are visually close to the GA. This is caused by a significant phase delay of the SF, which can be clearly seen in Fig. 6. The calculated RMSE of the GA estimate

obtained with the WF is 10–20% lower than the RMSE error of the KF; this means that the calculated values of the RMSE are more optimistic for all the conditions considered.

According to Table 3, the real RMSE of the WS exceeds that of the KS by no more than 8%, and the RMSE of the SS—by no more than 10%. It can be noted that there are much less differences between the RMSE of smoothers compared to usual filters, since there is no phase delay when smoothing algorithms are used. In this case, the calculated RMSE of the GA estimation with the WS is 10–20% lower than with the KS.

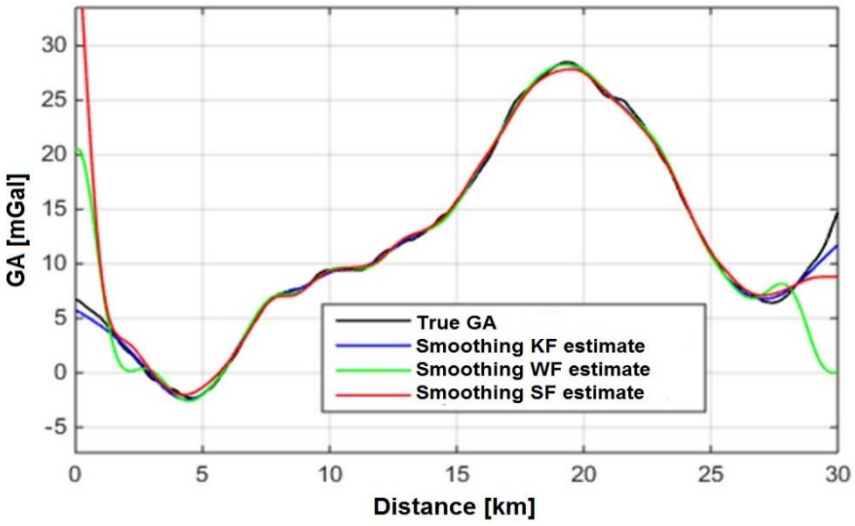

Fig. 7. GA estimates obtained with KS. WS and SS.

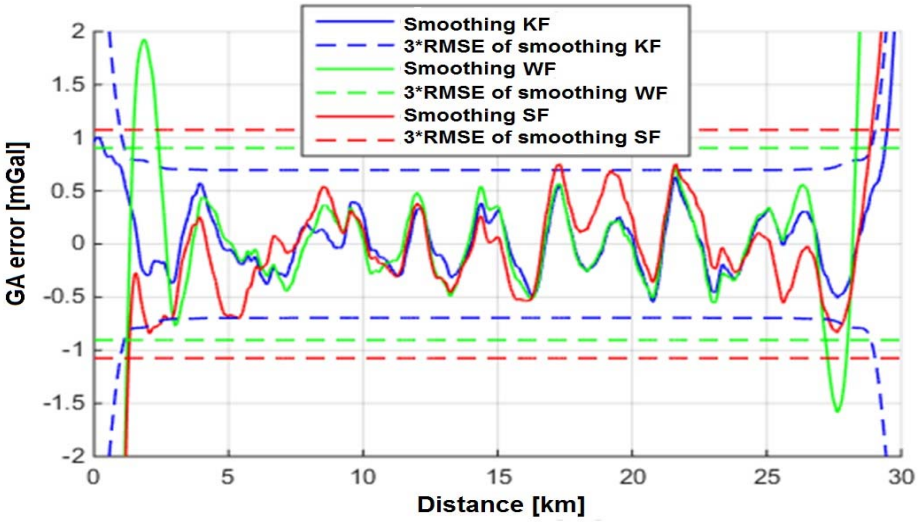

Fig. 8. GA smoothing errors for KS, WS and SS.

Table 2

RMSE of GA estimation with KF, WF and SF in steady-state mode

$\sigma_{\ddot{h}}$	1 mGal/km				2 mGal/km				3 mGal/km			
	KF	***WF (c)***	***WF (r)***	***SF (r)***	***KF***	***WF (c)***	***WF (r)***	***SF (r)***	***KF***	***WF (c)***	***WF (r)***	***SF (r)***
2 Gal	0.22	0.19	0.40	0.51	0.41	0.36	0.41	0.65	0.74	0.69	0.83	0.96
5 Gal	0.31	0.27	0.48	0.65	0.57	0.51	0.82	1.12	1.05	0.98	1.15	1.51
10 Gal	0.42	0.35	0.52	0.73	0.74	0.66	1.14	1.51	1.36	1.27	1.56	1.90
20 Gal	0.52	0.45	0.60	0.85	0.96	0.86	1.43	1.85	1.54	1.66	1.70	2.25

Note: *c* = calculated values, *r* = real values.

Table 3
RMSE of GA estimation with KS, WS and SS in steady-state mode

$\sigma_{\ddot{h}}$	1 mGal/km				2 mGal/km				3 mGal/km			
	KS	***WS (c)***	***WS (r)***	***SS (r)***	***KS***	***WS (c)***	***WS (r)***	***SS (r)***	***KS***	***WS (c)***	***WS (r)***	***SS (r)***
2 Gal	0.05	0.03	0.05	0.06	0.07	0.05	0.07	0.08	0.13	0.10	0.14	0.15
5 Gal	0.06	0.04	0.06	0.06	0.10	0.07	0.10	0.11	0.18	0.14	0.19	0.22
10 Gal	0.07	0.05	0.07	0.08	0.12	0.10	0.13	0.17	0.23	0.19	0.24	0.28
20 Gal	0.09	0.07	0.09	0.10	0.16	0.13	0.17	0.20	0.30	0.24	0.32	0.34

In absolute figures, the difference between the real values of the WF and KF RMSE does not exceed 0.15 mGal, and the difference between the real values of WS and KS RMSE does not exceed 0.05 mGal. Thus, the differences in models when using MLA to construct the WF slightly affect the real accuracy of the GA estimation, but negatively affect the consistency of the WF, which is understood as the consistency between the calculated and real accuracy characteristics of the filter [71]. In this sense, the KF is consistent because it is set for well-known models.

It can be noted that the RMSE of estimates obtained with the SS, especially for small values of standard deviation of the GA variability and vertical accelerations, also differ little from the RMSE of the optimal KS. However, the differences between the SF and KF are significant in the filtering mode. These results are further confirmed by real data processing. At the same time, it should be kept in mind that closeness of the RMSE noted above for various filters can be observed only for steady-state mode. During the transient process, the error of the WF and SF is noticeably higher than the RMSE of the KF.

It should also be emphasized that the KF and respective smoother will be optimal only for the specified models (2), (4) (which are assumed to be true in the simulation) and specific values of their parameters (which are known in the simulation conditions). In practice, when constructing the optimal filters within both the Wiener and Kalman approaches, there are some challenges related to the sensitivity to the models used and the values of their parameters if they differ from the real ones. In this case, it is necessary to synthesize adaptive filters, i.e. to estimate the GA and the model parameters simultaneously. To overcome these challenges, the methods developed within the Kalman approach can be effectively used, which is another important advantage [63, 72–746].

Next, we will compare the results obtained using the KF, WF and SF in the real data processing. For such a comparison, four pairs of return tacks (traversed in two mutually opposite directions) with different variability of GA and standard deviations of vertical accelerations were chosen in different areas of the World Ocean. The GA measurements were taken with a gyrostabilized gravimeter Chekan-AM. Two pairs of the chosen tacks with a small value of the GA variability (σ_{dga} = 0.5 mGal/km) were passed under strong ($\sigma_{\ddot{h}}$ = 40 Gal) (tacks 1, 2) and low ($\sigma_{\ddot{h}}$ = 10 Gal) (tacks 3, 4) waves. The other four tacks were selected in two areas with high GA variability (σ_{dga} = 3 mGal/km). Of these, the pair of tacks 5, 6 were surveyed with low waves ($\sigma_{\ddot{h}}$ = 10 Gal), and the tacks 7, 8—with strong ones ($\sigma_{\ddot{h}}$ = 40 Gal). Figure 9 shows an example of GA estimates obtained with the KF, WF and SF on tack 8, where the greatest difference between these filters can be observed. There is also the reference GA value in Fig. 9, obtained by averaging the estimates of the KS for all tacks, which demonstrates the phase delay of the SF.

Figure 10 shows the errors in the estimation with the KF, WF and SF.

Figure 11 depicts the GA estimates obtained with KS, WS and SS for the same tack, and the same reference is given for comparison. Figure 12 shows the estimation errors of smoothers.

To compare the accuracy of GA estimation with the KF and WF for each pair of return tacks 1–2, 3–4, 5–6, and 7–8, the real (r) RMSE were calculated according to the difference in the GA estimates between these filters in steady-state mode. These RMSE are given in Table 4 along with the calculated (c) values of the RMSE. The latter were found for the KF by means of the covariance matrix calculated in the KF, and for the WF they were calculated by (18), (19).

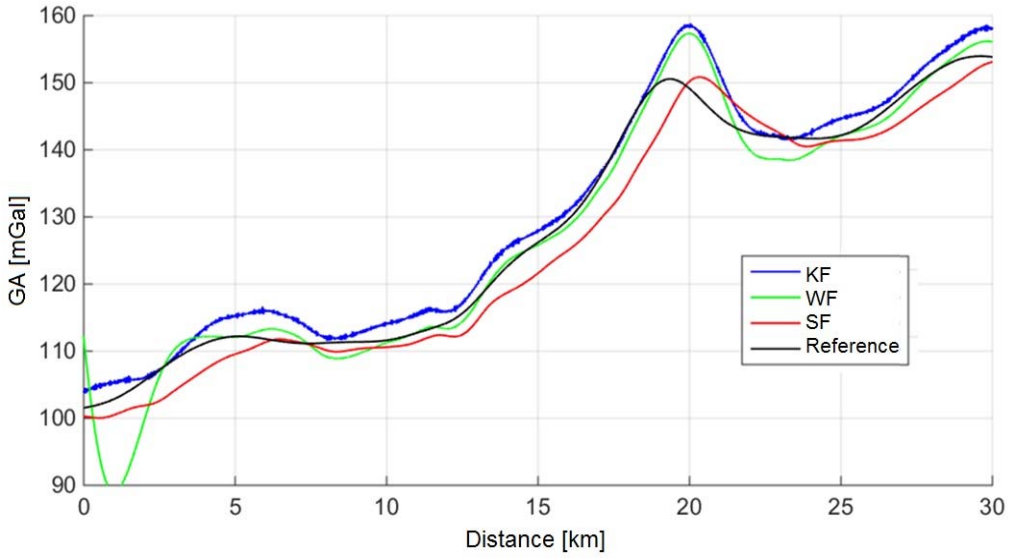

Fig. 9. GA estimates obtained with the KF, WF and SF.

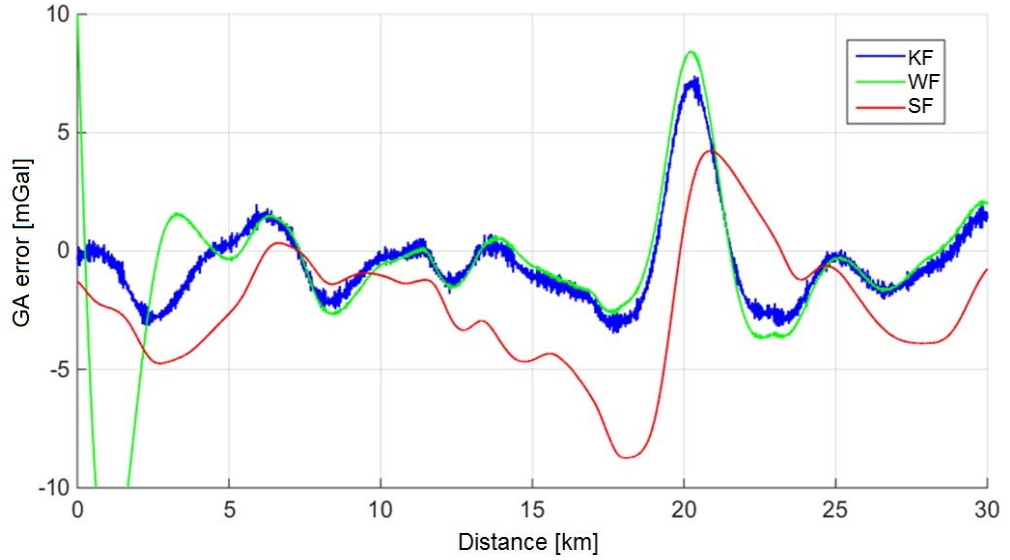

Fig. 10. GA filtering errors for the KF, WF and SF.

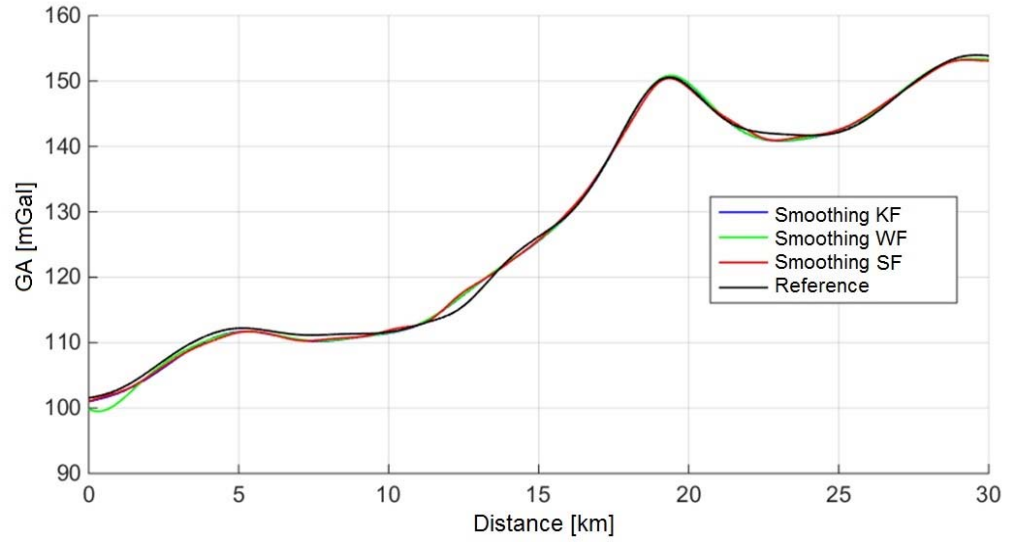

Fig. 11. GA estimates obtained with KS, WS and SS.

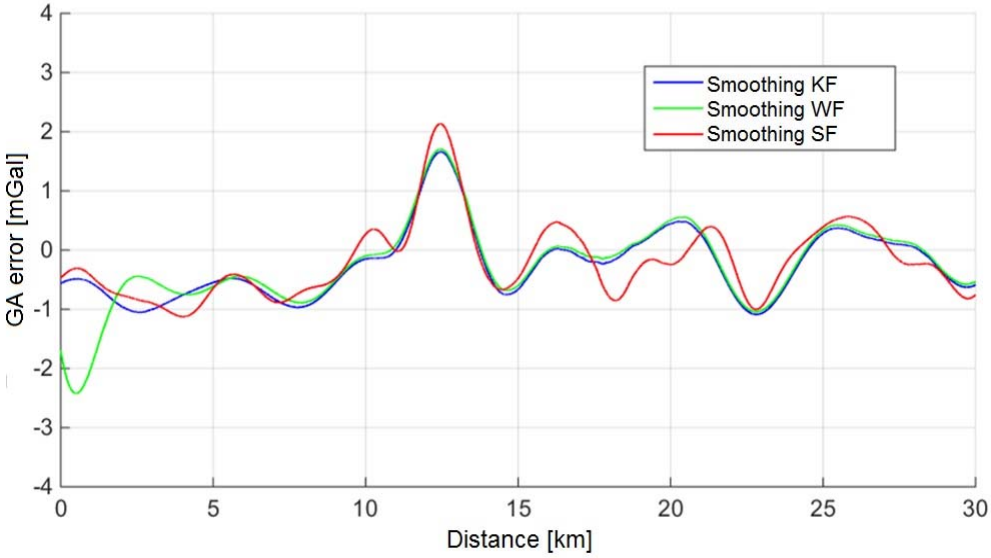

Fig. 12. GA smoothing errors for KS, WS and SS.

Table 4
RMSE of GA estimation with KF, WF and SF

Tacks	Smoothing					Filtering				
	KF (c)	***KF (r)***	***WF (c)***	***WF (r)***	***SF (r)***	***KF (c)***	***KF (r)***	***WF (c)***	***WF (r)***	***SF (r)***
1-2	0.04	0.02	0.02	0.02	0.03	0.20	0.14	0.16	0.15	0.34
3-4	0.08	0.07	0.06	0.10	0.28	0.51	0.36	0.43	0.53	0.68
5-6	0.12	0.34	0.09	0.41	0.34	0.78	0.73	0.63	0.90	1.33
7-8	0.26	0.80	0.20	0.81	0.81	1.44	1.56	1.20	1.74	3.89

It follows from the above results that the KF, WF and SF have close real RMSE of estimation, which correlates well with the predictive simulation results. The calculated and real RMSE of GA estimation with the KF and WF are close only for the tacks with low GA variability, which indicates the consistency of these filters in the given conditions. For the tacks with high GA variability, the difference between the calculated and real RMSE is significant (up to 0.6 mGal), which is especially apparent on tacks 7–8 with high vertical accelerations. This fact suggests that it is advisable to refine the model of measurement errors in the given conditions.

CONCLUSIONS

The interrelation, differences and features of algorithms for processing the results of marine scalar gravimetric surveys (filters), synthesized within the Kalman and Wiener approaches have been discussed. Their advantages and disadvantages in solving the filtering and smoothing problems have been studied, and the features of the GA estimation problems solved on a marine moving vehicle have been considered in comparison with similar problems for aircraft.

The results obtained with different filters in predictive simulation and real data processing have been presented and compared. The consistency of the Kalman filters in case of low values of the GA gradient has been confirmed. However, in some cases the consistency was found to be unsatisfactory, which means that the models of the useful signal (GA) and interference (vertical inertial accelerations) need to be refined in the given conditions.

The differences between filters and smoothers related to the presence/absence of delay have been shown, and it has been noted that there is a significant, up to 7-fold decrease in the GA estimation errors in the smoothing mode compared to the filtering mode.

As expected, the results of the research showed that the main advantages of the KF compared to the WF and respective smoothers in determining the GA are shorter transients and the possibility to calculate

the current accuracy characteristics. Another advantage of the Kalman approach application to this problem is a relatively simple way of generalization if additional measurements are involved, which is quite important in the integrated processing of gravimeter and GNSS data [63, 64].

The WF built for the same models as the KF, provides the same accuracy in steady-state mode, but has a longer transient process and cannot generate the current accuracy characteristic.

It has been emphasized that, when constructing the optimal filters within both the Wiener and Kalman approaches, there are certain problems with sensitivity to the models of useful signal and interference, so there is the need for adaptive filters synthesis. To overcome these problems, the algorithms developed within the Kalman approach can be effectively used, since they provide for the GA estimation and model parameters identification simultaneously, which is another important advantage of this approach [63, 72, 73]. However, these issues are beyond the scope of this work and should be considered in a separate study. Moreover, it is important to continue studying the use of GNSS high-precision measurements in marine gravimetric surveys with the aim to expand the potential conditions for these activities.

FUNDING

This work was supported by the Russian Science Foundation grant No. 23-19-00626, https://rscf.ru/project/23-19-00626/.

CONFLICT OF INTEREST

The authors of this work declare that they have no conflicts of interest.

REFERENCES

1. Schwarz, K.P., Inertial surveying and geodesy, Reviews of Geophysics and Space Physics, 1983, vol. 21(4), 878–890.
2. Panteleev, V.L., Lineinaya fil'tratsiya v zadachakh dinamicheskoi gravimetrii (Linear Filtering in the Problems of Dynamuc Gravimetry), Moscow: MGU, 1985.
3. Torge, W., Gravimetry, Berlin: de Gruyter, 1989.
4. Panteleev, V.L., Fil'tratsiya v zasachakh inertsial'noi gravimetrii (Filtering in Inertial Gravimetry), LAP LAMBERT Academic Publishing, 2012.
5. Bolotin, Yu.V. and Golovan, A.A., Methods of inertial gravimetry, Moscow University Mechanics Bulletin, 2013, vol. 68, no. 5, pp. 117–125.
6. Peshekhonov, V.G., Stepanov, O.A., Avgustov, L.I., et al., Methods and Technologies for Measuring the Earth's Gravity Field Parameters, V.G. Peshekhonov, O.A. Stepanov, Eds., Springer, 2022, https://doi.org/10.1007/978-3-031-11158-7
7. Peshekhonov, V.G., Stepanov, O.A., Rozentsvein, V.G., Krasnov, A.A., and Sokolov, A.V., State-of-the-art strapdown airborne gravimeters: Analysis of the development, Gyroscopy and Navigation, 2022, vol. 13, no. 4, pp. 3–35, https://doi.org/10.1134/S2075108722040101
8. Jekeli, C., Kwon, J.H., Results of airborne vector (3-D) gravimetry, Geophysical Research Letters, 1999, vol. 26(23), pp. 3533–3536.
9. Vyaz'min, V.S., Golovan, A.A., and Bolotin, Yu.V., The journey from scalar to vector airborne gravimetry, in: 110 Let so dnya rozhdeniya akademika A.Yu. Ishlinskogo (110th Anniversary of Academician A.Yu. Ishlinskii), Collection of papers, St. Petersburg: Mediapapir, 2023, pp. 105–117.
10. Wiener, N., The Interpolation, Extrapolation and Smoothing of Stationary Time Series, New York: J. Wiley, 1949.
11. Andreev, N.I., Korrelyatsionnaya teoriya statisticheski optimal'nykh sistem (Correlation Theory of Statistically Optimal Systems), Moscow: Nauka, 1966.
12. Chelpanov, I.B., Optimal'naya obrabotka signalov v navigatsionnykh sistemakh (Optimal Processing of Signals in Navigation Systems), Moscow: Nauka, 1967.
13. Chelpanov, I.B., Nesenyuk, L.P., and Braginskii, M.V., Raschet kharakteristik navigatsionnykh giropriborov (Calculation of Characteristics of Navigation Gyrodevices), Leningrad: Sudostroenie, 1978.
14. Shakhtarin, B.I., Fil'try Vinera i Kalmana (Kalman and Wiener Filters), Moscow: Golos ARV, 2008.
15. Kalman, R. E., Bucy R. S., New results in linear filtering and prediction theory, Transactions of the ASME – Journal of Basic Engineering, 1961, vol. 83(1), pp. 95–107.
16. Rivkin, S.S., Ivanovskii, R.I., and Kostrov, A.V., Statisticheskaya optimizatsiya navigatsionnykh sistem (Statistical Optimization of Navigation Systems), Leningrad: Sudostroenie, 1976.
17. Dmitriev, S.P., Vysokotochnaya morskaya navigatsiya (High-Precision Marine Navigation), St. Petersburg: Sudostroenie, 1991.
18. Stepanov, O.A., Osnovy teorii otsenivaniya s prilozheniyami k zadacham obrabotki navigatsionnoi informatsii (Fundamentals of the Estimation Theory with Applications to the Problems of Navigation Information Processing), Part 1, Vvedenie v teoriyu otsenivaniya (Introduction to the Estimation Theory), St. Petersburg: Concern CSRI Elektropribor, 2017.
19. Stepanov, O.A., Osnovy teorii otsenivaniya s prilozheniyami k zadacham obrabotki navigatsionnoi informatsii (Fundamentals of the Estimation Theory with Applications to the Problems of Navigation Information Processing), Part 2, Vvedenie v teoriyu fil'tratsii (Introduction to the Filtering Theory), St. Petersburg: Concern CSRI Elektropribor, 2017
20. Bolotin, Yu.V., Golovan, A.A., and Parusnikov, N.A., Uravneniya aerogravimetrii. Algoritmy i rezul'taty ispytanii (Airborne Gravimetry Equations. Test Algorithms and Results), Moscow: Moscow State University Publisher, 2002.

21. Rudenko, E.A., Comparison of stochastic filtering algorithms, Proc. XXXII Conference in Memory of N.N. Ostryakov, St. Petersburg, 2020, pp. 295–299.
22. Tikhonov, V.I., Kharisov, V.N., Statisticheskii analiz i sintez radiotekhnicheskikh ustroistv i sistem (Statistical Analysis and Synthesis of Wireless Devices and Systems), Textbook, 3rd Ed., Moscow: Goryachaya liniya–Telekom, 2018.
23. Stratonovich, R.L., Conditional Markov processes, Teoriya veroyatnosti i ee primeneniye, 1960, vol. 5, no. 2, pp. 172–195.
24. Stratonovich, R.L., Theory of Markov processes, applied to optimal filtering of signals, Radiotekhnika i elektronika, 1960, vol. 5, no. 11, pp. 1751–1763.
25. Rauch, H.E., Tung, F., and Striebel, C.T., Maximum likelihood estimates of linear dynamic systems, The American Institute of Aeronautics and Astronautics Journal, 1965, vol. 8, no. 3, pp. 1445–1450.
26. Stepanov, O.A., Relations of algorithms of optimal stationary filtering and smooting, Giroskopiya i navigatsiya, 2004, no. 1, pp. 16–27.
27. Bolotin Y.V., Yurist S.S., Suboptimal smoothing filter for the marine gravimeter GT-2M, Gyroscopy and Navigation, 2011, vol. 2, no. 3, pp. 152–155.
28. Sarkka, S., Bayesian Filtering and Smoothing, Cambridge University Press, 2013. doi: 10.1017/CBO9781139344203.
29. Popov, E.I., Opredelenie sily tyazhesti na podvizhnom osnovanii s pomoshch'yu sil'no dempfirovannykh gravimetrov (Gravity Measurement Using Highly Damped Gravimeters on Moving Carrier), Moscow: Nauka, 1967.
30. Ogorodova, L.V., Shimbirev, B.P., and Yuzefovich, A.P., Gravimetriya (Gravimetry), Moscow: Nedra, 1978.
31. Panteleev, V.L., Osnovy morskoi gravimetrii (Fundamentals of Marine Gravimetry), Moscow: Nedra, 1983.
32. Nabighian, M.N., Ander, M.E., Grauch, V.J.S., Hansen, R.O., LaFehr, T.R., Li, Y., Pearson, W.C., Peirce, J.W., Phillips, J.D., and Ruder, M.E., Historical development of the gravity method in exploration, Geophysics, 2005, vol. 70, no. 6, pp. 63–89.
33. Peshekhonov, V.G., Sokolov, A.V., Zheleznyak, L.K., Bereza, A.D., and Krasnov, A.A., Role of navigation technologies in mobile gravimeters development, Gyroscopy and Navigation, 2020, vol. 11, no. 1, pp. 2–12.
34. Hein, G.W., Progress in airborne gravimetry: Solved, open and critical problems, in: Proc. of the IAG Symposium on Airborne Gravity Field Determination, IUGG XXI General Assembly Boulder, Colorado, USA, 1995, pp. 3–11.
35. Childers, V.A., Bell, R.E., and Brozena, J.M., Airborne gravimetry: An investigation of filtering, Geophysics, 1999, vol. 64, pp. 61–69.
36. Kwon, J.H., Jekeli, C., A new approach for airborne vector gravimetry using GPS/INS, J. Geod., 2001, vol. 74, pp. 690–700, doi: 10.1007/s001900000130.
37. Hannah, J., Airborne Gravimetry: a Status Report. Prepared for the Surveyor, General Land Information, Otago University, New Zealand, 2001.
38. Jekeli, C., Theoretical Fundamentals of Airborne Gradiometry, Airborne Gravity for Geodesy Summer School, 23–27 May, 2016.
39. Becker, D., Advanced calibration methods for strapdown airborne gravimetry, Ph.D. Thesis, Technische Universität Darmstadt, 2016.
40. Golovan, A.A., Vyaz'min, V.S., Methodology of airborne gravimetry surveying and strapdown gravimeter data processing, Gyroscopy and Navigation, 2023, vol. 14, no. 1, pp. 36–47, DOI:10.1134/S2075108723010029
41. Levitskaya, Z.N., Optimal linear algorithms for filtering the gravity at sea based on experimental data, Candidate of Science (Engineering) Dissertation, Moscow: Izdatel'stvo MGU, 1972.
42. Masalov, I.A., Dinamicheskaya gravimetriya (Dynamic Gravimetry), Moscow: Nauka, 1983..
43. Bereza, A.D., Kostrov, A.V., and Rivkin, S.S., Study of filtering methods for gravimetric surveys, in: Fizikotekhnicheskaya gravimetriya (Physico-technical Gravimetry), V.I. Strakhov, Ed., Moscow: Nauka, 1982, pp. 61–88.
44. Volkov, A.S., Capabilities of dynamic systems with delay in marine gravimetry, in: Lineinaya fil'tratsiya v zadachakh dinamicheskoi gravimetrii (Linear Filtering in the Problems of Marine Gravimetry), V.L. Panteleev, Ed., Moscow: Izdatel'stvo MGU, 1985, pp. 14–22.
45. Peshekhonov, V.G., Nesenyuk, L.P., Starosel'tsev, L.P., and Elinson, L.S., Sudovye sredstva izmereniya parametrov gravitatsionnogo polya Zemli (Shipborne Aids Measuring the Parameters of the Earth's Gravity Field), Leningrad: Rumb, 1989.
46. Yurist, S.Sh., Smoller, Yu.L., Il'in, V.L., and Volnyanskii, V.N., A small-sized marine gravimerer, Proc. 2nd International Conference "Marine and Airborne Gravimetry", St. Petersburg, 1994.
47. Vol'fson, G.V., Primenenie graviinertsial'nykh tekhnologii v geofizike (Intertial Gravimetric Technology Application to Geophysics), V.G. Peshekhonov, Ed., Concern CSRI Elektropribor, JSC, 2002.
48. Zheleznyak, L.K., Koneshov, V.N., Peshekhonov, V.G., Nesenyuk, L.P., Elinson, L.S., Il'in, V.N., Chichinadze, M.V., Bronshtein, I.G., Knyazev, Yu.A., and Parusnikov, N.A., Dual usage gravimeters for measurements onboard marine and airborne vehicles, Izvestiya vuzov. Priborostroenie, 2005, vol. 48, no. 5, pp. 23–28.
49. Drobyshev, N.V., Zheleznyak, L.K., Klevtsov, V.V., Koneshov, V.N., and Solov'ev, V.N., Techniques and problems related to studies of the world ocean gravity field, Geofizicheskie issledovaniya, 2006, no. 5, pp. 32–52.
50. Koneshov, V.N., Modern methods of marine and airborne gravimetry developed with participation of the Institute of Physics of the Earth of The Russian Academy of Sciences, Zemlya i Vselennaya, 2018, no. 6, pp. 13–20.
51. Ivanovskii, R.I., Some aspects of development and application of stationary filters to navigation systems, Gyroscopy and Navigation, 2012, vol. 3, no. 1, pp. 102–114.
52. Loparev, A.V., Stepanov, O.A., and Chelpanov, I.B., Using frequency approach to time-variant filtering for processing of navigation information, Gyroscopy and Navigation, 2012, vol. 3, no. 1, pp. 9–19.

53. Zinenko, V.M., Application of suboptimal time-invariant filters, Gyroscopy and Navigation, 2012, vol. 3, no. 4, pp. 286–297.
54. Stepanov, O.A., Blazhnov, B.A., and Koshaev, D.A., Studying the effectiveness of using satellite measurements in airborne gravity determination, Giroskopiya i navigatsiya, 2002, no. 3 (38), pp. 33–47.
55. Stepanov, O.A., Motorin, A.V., Koshaev, D.A., Sokolov, A.V., and Krasnov, A.A., Comparison of stationary and nonstationary adaptive filtering and smoothing algorithms for gravity anomaly estimation on board the aircraft, Proc. 4th IAG Symposium on Terrestrial Gravimetry: Static and Mobile Measurements (TG-SMM-2016), St. Petersburg, 2016, pp. 53–60.
56. Sokolov, A.V., Stepanov, O.A., Krasnov, A.A., and Motorin, A.V., Comparison of Wiener and Kalman filters in processing the results of marine gravimetric survey, Proc. 30th Saint Petersburg International Conference on Integrated Navigation Systems, St. Petersburg, 2023, pp. 62–68. DOI:10.23919/ICINS51816.2023.10168435
57. Bolotin, Yu.V. and Vyaz'min, V.S., Gravity anomaly estimation by airborne gravimetry data using LSE and minimax optimization and spherical wavelet expansion, Gyroscopy and Navigation, 2015, vol. 6, no. 4, pp. 310–317.
58. Krasnov, A.A. and Sokolov, A.V., A modern software system of a mobile Chekan-AM gravimeter, Gyroscopy and Navigation, 2015, vol. 6, no. 4., pp. 278–287.
59. Jordan, S.K., Self-consistent statistical models for gravity anomaly and undulation of the geoid, Journal of Geophysical Research, 1972, vol. 77/(20), pp. 2156–2202.
60. Loparev, A.V., Optimization of algorithms for measuring the profile of sea waves, Cand. of Science (Engineering) Dissertation, St. Petersburg: GUAP, 2001.
61. Sokolov, A.V., Krasnov, A.A., and Zheleznyak, L.K., Improving the accuracy of marine gravimeter, Gyroscopy and Navigation, 2019, vol. 10, no. 3, pp. 155–160. https://doi.org/10.1134/S2075108719030088
62. Stepanov, O.A., Loparev, A.V., and Chelpanov, I.B., Time-and-frequency approach to navigation information processing, Automation and Remote Control, 2014, vol. 75, no. 6, pp. 1090–1108.
63. Stepanov, O.A., Koshaev, D.A., Motorin, A.V., Krasnov, A.A., and Sokolov, A.V., Algorithms for integrated processing of marine gravimeter data and GNSS measurements, IFAC-PapersOnLine, 2020, vol. 53, no. 2, pp. 500–505.
64. Sokolov, A.V., Motorin, A.V., Stepanov, O.A., Koshaev, D.A., and Krasnov, A.A., Using high-precision satellite measuremenets to solve the problem of marine gravimetric surveys, Proc. 27th St. Petersburg International Conference on Integrated Navigation Systems, 2020. DOI:10.23919/ICINS43215.2020.9133743
65. Cai, S., Tie, J., Zhang, K., Cao, J., and Wu, M., Marine gravimetry using the strapdown gravimeter SGAWZ, Marine Geophysical Research, 2017, vol. 38, no. 4, pp. 325–340, doi:10.1007/s11001-017-9312-9.
66. Wang, W., Gao, J., Li, D., Zhang, T., Luo, X., and Wang, J., Measurements and accuracy evaluation of a strapdown marine gravimeter based on inertial navigation, Sensors, 2018; vol. 18(11), p. 3902, https://doi.org/10.3390/s18113902.
67. Sergienko, A.B., Tsifrovaya obrabotka signalov (Digital Processing of Signals), 3rd Ed., St. Petersburg: BHV-Peterburg, 2011.
68. Fairhead, J.D., Odegard, M.E., Advances in gravity survey resolution, The Leading Edge, 2002, vol. 21, pp. 36–37.
69. Devaraju, B., Sneeuw, N., On the spatial resolution of homogeneous isotropic filters on the sphere, Proc. VIII Hotine-Marussi Symposium on Mathematical Geodesy, 2015, pp. 67–73, https://doi.org/10.1007/1345_2015_5
70. Jensen, T.E., Spatial resolution of airborne gravity estimates in Kalman filtering. Journal of Geodetic Science, 2022, vol. 12, no. 1, pp. 185–194. https://doi.org/10.1515/jogs-2022-0143
71. Stepanov, O.A., Isaev, A.S., A procedure of comparative analysis of recursive nonlinear filteringt algorithms in navigation data processing based on predictive simulation, Gyroscopy and Navigation, 2023, vol. 14, no. 4, pp. 213–224.
72. Motorin, A.V., Stepanov, O.A. Designing an error model for navigation sensors using the Bayesian approach, Proc. IEEE International Conference on Multisensor Fusion and Integration for Intelligent Systems, 2015, pp. 54–58.
73. Stepanov, O.A., Koshaev, D.A., and Motorin, A.V., Identification of gravity anomaly model parameters in airborne gravimetry problems using nonlinear filtering methods, Gyroscopy and Navigation, 2015, vol. 6, no. 4, pp. 318–323.
74. Motorin, A.V., Nosov, A.S., Accuracy and sensitivity analysis for marine gravimetry algorithms in dependence of survey conditions, Proc. 2019 IEEE Conference of Russian Young Researchers in Electrical and Electronic Engineering (ElConRus 2019), 2019, pp. 1210–1215, doi: 10.1109/EIConRus.2019.8656640.